# NUMERICAL CALCULATIONS OF PRESSURE OSCILLATIONS IN A SIDE-DUMP RAMJET ENGINE

V. Yang* and F. E. C. Culick**
California Institute of Technology
Pasadena, California

## ABSTRACT

Pressure oscillations in a side-dump ramjet engine have been studied, using a one-dimensional numerical analysis. The engine is treated in two parts: the inlet section, including a region of two-phase flow downstream of fuel injection, and a dump combustor. Each region is treated separately and matched with the other. Following calculation of the mean flow field, the oscillatory characteristics of the engine are determined by its reponse to a disturbance imposed on the mean flow. Results have shown favorable comparison with experimental data obtained at the Naval Weapons Center, China Lake.

## NOMENCLATURE

| | |
|---|---|
| $A$ | cross-sectional area |
| $c_l$ | specific heat of fuel |
| $c_p$ | constant pressure specific heat of air |
| $f$ | frequency |
| $F_p$ | drag force between air and fuel droplets |
| $h$ | enthalpy |
| $K$ | heat conduction coefficient of air |
| $L$ | latent heat of liquid fuel |
| $L_f$ | position coordinate of fuel injector |
| $M$ | Mach number |
| $\dot{m}_{k,i}$ | rate of consumption of ith species |
| $p$ | pressure |
| $Q_p$ | heat transfer rate between air and fuel droplets |
| $R$ | gas constant |
| $r_b$ | surface regression rate of droplet |
| $r_p$ | radius of droplet |
| $t$ | time |
| $T$ | temperature |
| $u$ | velocity |
| $V$ | volume of stirred reactor |
| $x$ | position coordinate along the axis of the engine, normalized w.r.t. the inlet length |
| $Y_i$ | mass fraction of ith species |
| $\chi$ | gas constant, normalized w.r.t. that of the air |
| $\gamma$ | ratio of specific heats |
| $\mu$ | viscosity |
| $\nu$ | stoichiometric coefficient |
| $\dot{\omega}_f$ | rate of consumption of fuel in the stirred reactor |
| $\omega_p$ | rate of liquid fuel injected into the main flow |
| $\varphi$ | equivalence ratio |
| $\rho$ | density |
| $\rho_l$ | density of liquid fuel |
| $\sigma_l$ | surface tension of liquid fuel |
| $\Delta H$ | heat of combustion per unit mass of fuel |

subscripts

| | |
|---|---|
| $p$ | liquid phase |
| $sg$ | value at port of fuel injector |
| 1 | value at the exit plane of the inlet |
| 2 | value at the inlet plane of the combustor |
| 3 | value at the exit plane of the stirred reactor |

## I. INTRODUCTION

Recent developments in liquid-fueled ramjet engines have experienced serious difficulties with pressure oscillations - called generically combustion instabilities.[1] They are a consequence of the complicated interactions between acoustic waves, combustion processes, and mean flowfields. If compensating influences acting to attenuate the oscillations are weak, then unsteady motions in the flowfield may reach sufficient amplitude to interfere with proper operation.

Several modes of oscillations have been observed. They are classified as bulk, longitudinal, and transverse modes according to the frequency range and spacial structure. The low frequency longitudinal oscillation seems to be most troublesome. It may interact with the inlet shock structure and reduce the stability margin of the inlet system. The purpose of this paper is to examine the unsteady behaviors of a side-dump ramjet engine within the low frequency range, using a numerical analysis.

Analytical treatments of low frequency combustion instabilities in liquid-fueled ramjet engine have been carried out by several groups. All these models are based on linear perturbation methods, giving results valid in the limit of small amplitudes. Culick and Rogers[2] gave probably the first detailed analysis of the stability of low frequency oscillations in ramjet engines with both inlet and dump combustor

---

* Graduate Student

** Professor of Applied Physics and Jet Propulsion, Associate Fellow AIAA

accounted for. Some formulas were given for the frequencies and mode shapes approximating the oscillations which had been observed in two engines. The combustion processes were accommodated in a crude fashion, not treated in detail. Later, Yang and Culick[3] presented a one-dimensional analysis using an integral formulation. The combustion zone and the shear layer were represented by a thin flame sheet and a dividing streamline respectively. Their instantaneous motions were calculated as a part of the solution. Reardon[4] applied a combustion time lag model, originally developed for dealing with bulk oscillations in liquid propellant rockets, to the corresponding ramjet problems. In reference 5, the rumble oscillations in a coaxial dump combustor have been investigated with attention focused on the interplays of entropy and acoustic waves. The acoustic field in the inlet is represented by a leftward traveling wave, the reflection process of the shock being ignored.

The work described here is directed specifically to studying the flowfields in a research side-dump ramjet engine operated at the Naval Weapons Center (China Lake).[6,7] Figure 1, taken from reference 7, shows the baseline configuration considered. Preheated air is delivered from the plenum chamber to the combustor through two circular side ducts. Fuel injection takes place just behind the diffuser section to ensure adequate mixing of air and droplets, using a fixed orifice, contra-stream injection system. Because the engine exhibits severe transverse oscillations under many test conditions, a tangential mode suppression vane is used. This has proved to be an effective method, suppressing high frequency fluctuations significantly. Details of the system are given in reference 6.

In the following sections, a one-dimensional model is employed to formulate the problem, which is then solved numerically. The engine is treated in two parts: the inlet section, including a region of two-phase flow downstream of the plane of fuel injection, and the dump combustor. Combustion processes are crudely modeled as a stirred reactor, occupying the forward portion of the combustor, followed by a length of plug flow. Calculations are first carried out for the steady flowfields. The unsteady behavior of the engine is then determined by its response to a small disturbance imposed on the mean flow. In addition to the spacial distributions of amplitude and phase, the power spectral density is computed for the time history of the pressure.

## II. FORMULATION

Because the flow properties change abruptly across the dump plane, the engine is first approximated by division into two parts: the inlet section (region I) and the dump combustor. Each region is treated separately and matched with the other. The physical phenomena downstream of the inlet ports, roughly ranging from the dome of the combustor to the tranverse mode suppression vane, are extremely complicated, involving mixing of unburned and burned gases, droplet vaporization, and finite-rate chemical reaction. To bypass these complexities, a lumped parameter analyis is used to formulate the combustion processes in this region. The combustor therefore consists of a stirred reactor section (region II) for ignition and preliminary combustion, and a plug flow reactor section (region III) for final burn-out.

The analysis is based on a one-dimensional model for two phase flow, being developed by considering the balances of flow properties in the gas and the liquid phases respectively. If we neglect viscous effects and assume the fuel droplets are uniformly distributed over the entire cross-sectional area, the equations governing the flow in each phase can be written in the following conservation and non-conservation forms.

gas-phase mass equation

$$\frac{\partial \rho}{\partial t} + \frac{1}{A}\frac{\partial(\rho u A)}{\partial x} = 3\rho_p r_b \tag{1}$$

gas-phase momentum equation

$$\frac{\partial(\rho u)}{\partial t} + \frac{1}{A}\frac{\partial}{\partial x}\left[\left(\frac{p}{\gamma_{in}} + \rho u^2\right)A\right] = \frac{p}{\gamma_{in}A}\frac{dA}{dx} + F_p + 3\rho_p r_b u_p \tag{2}$$

gas-phase energy equation

$$\frac{\partial}{\partial t}\left[\rho\left(\frac{\chi T}{\gamma_{in}(\gamma-1)} + \frac{u^2}{2}\right)\right] + \frac{1}{A}\frac{\partial}{\partial x}\left[\rho u A\left(\frac{\chi T}{\gamma_{in}(\gamma-1)} + \frac{u^2}{2}\right)\right] = \frac{-1}{\gamma_{in}A}\frac{\partial(upA)}{\partial x} + \frac{Q_p}{\gamma-1} + u_p F_p + 3\rho_p r_b\left(h_v + \frac{u_p^2}{2}\right) + \dot{m}_{k,f}\Delta H \tag{3}$$

species equation

$$\frac{\partial(\rho Y_i)}{\partial t} + \frac{1}{A}\frac{\partial(\rho Y_i u A)}{\partial x} = -\dot{m}_{k,i} + \theta\times 3\rho_p r_b \qquad i = o, f;\ \theta = 0 \text{ if } i = o \tag{4}$$

liquid-phase mass equation

$$\frac{\partial \rho_p}{\partial t} + \frac{\partial(\rho_p u_p)}{\partial x} = \omega_p - \frac{\rho_p u_p}{A}\frac{dA}{dx} - 3\rho_p r_b \tag{5}$$

liquid-phase momentum equation

$$\frac{\partial u_p}{\partial t} + u_p\frac{\partial u_p}{\partial x} = -\frac{F_p}{\rho_p} \tag{6}$$

liquid-phase energy equation

$$\frac{\partial T_p}{\partial t} + u_p\frac{\partial T_p}{\partial x} = -\frac{Q_p}{\rho_p c_l} \tag{7}$$

The flow properties are normalized with respect to their quantities at the end of the inlet diffuser except the velocity, which is referenced to the speed of sound. Note that the mass source term $\omega_p$ is introduced only at the injector position ($x=L_p$). The energy equation for the liquid phase (7) is valid only for the subcooled droplets, accounting for the initial heating-up processes. The fuel evaporized in this period is ignored. As soon as the droplets reach their saturated states, that equation is replaced by a formula for the surface regression rate written in the Lagrangian coordinate.

$$\frac{Dr_p}{Dt} = r_b \tag{8}$$

In this study, the fuel/air mixture is lean and well

fixed before evaporization occurs. Each droplet acts individually without interaction with the others. The radius $r_b$ is therefore obtained by considering the vaporization or combustion of a single droplet in a convective environment.

To complete the formulation, the empirical correlations for the initial droplet size, drag force, heat transfer rate, and the droplet regression rate are required. The relevant relations used to simulate the typical flow conditions are given in Table 1.

Table 1. Empirical correlations

| *Correlation* | *Reference* |
|---|---|
| *droplet diameter* | *Hussein*[8] |
| *drag force* | *Dickerson* and *Schuman*[9] |
| *convective heat transfer* | *Rowe* and *Claxton*[10] |
| *regression rate of droplet* | |
| *pure vaporization* | *Glassman*[11] |
| *droplet combustion* | *Glassman*[11] |

**Combustion Process**

The chemical reaction rate $\dot{m}_{k,i}$ is an essential element in the entire analysis. Its formulation depends strongly on the conditions of the droplets flowing into the combustor. A simple estimate of the droplet size in the inlet section has been made by comparing various time scales associated with the droplet heating-up, the vaporization rate, and the flow residence. For the problem studied here, most of the vaporization takes place within the inlet, producing very tiny droplets with diameter of the order of 10 microns at the dump plane. As a result, the combustion processes are assumed to be homogeneous,[12] similar to those of a premixed combustible gas. Further check of this assumption will be given later.

As mentioned earlier, the flowfield in the upstream part of the combustor is treated as a stirred reactor in which chemical reaction takes place uniformly. While the method provides reasonable solutions for the energy release, direct application of it to unsteady problems is inappropriate. The reactor usually occupies such a space that prohibits certain spacial variations of oscillatory flowfields. Consequently, the frequencies may be overestimated except for very low frequency oscillations.

To get around this problem, a patching technique has been used with the consideration of an equivalent combustor as shown in Figure 2. The flowfield is assumed to be quasi one-dimensional everywhere in the combustion chamber. However, the rate of heat generation due to combustion in the stirred reactor section is calculated in an average sense, using a lumped parameter analysis described below.

Conservation laws are applied to obtained three conservation equations together with two species equations. Legitimately, these equations can be derived by integrating (1)-(4) with respect to x over the reactor section and ignoring the momentum and heat transfer between two phases.

$$V\frac{d\rho}{dt} = \dot{m}_1 - \dot{m}_3 \tag{9}$$

$$V\frac{d\rho u}{dt} = \dot{m}_1 u_1 - \dot{m}_3 u_3 + A_2(p_1 - p_2) \tag{10}$$

$$V\frac{d\rho E}{dt} = \dot{m}_1 h_{t1} - \dot{m}_3 h_{t3} + \dot{\omega}_f \Delta H \tag{11}$$

$$V\frac{d\rho Y_f}{dt} = \dot{m}_1 Y_{f1} - \dot{m}_3 Y_{f3} - \dot{\omega}_f \tag{12}$$

$$V\frac{d\rho Y_o}{dt} = \dot{m}_1 Y_{o1} - \dot{m}_3 Y_{o3} - \nu\dot{\omega}_f \tag{13}$$

The subscripts 1 and 3 denote respectively the inlet and the exit planes of the reactor, and $Y_{f1}$ is the bulk mass fraction of the fuel at the entrance, including both fuel vapor and droplet. The chemical reaction rate $\dot{\omega}_f$ is determined with a global chemical kinetic model proposed by Edelman and Fortune.[13]

$$\dot{\omega}_f = \alpha' T^n p^{0.3} p^{1.5} e^{\frac{-E}{RT}} Y_f^{0.5} Y_o \equiv \alpha Y_f^{0.5} Y_o \tag{14}$$

Rearrangement of Eqs. (12), (13), and (14) produces a third-order polynominal for $Y_{f3}$.

$$d_3 Y_{f3}^3 + d_2 Y_{f3}^2 + d_1 Y_{f3} + d_0 = 0 \tag{15}$$

where the coefficients $d_i$ are functions of the flow properties and the inlet fuel concentration.

The overall calculation for the chemical reaction rate $\dot{\omega}_f$ is based on an iteration scheme. We first assume the temperature field in the reactor and compute $Y_{f3}$ from (15), taking the pressure field to be $p_1$. $\dot{\omega}_f$ is then determined from (14). As a result, the flow properties in the reactor become known after some manipulations of (9)-(11). The same procedure is repeated until the calculated temperature converges to its initial guessed value. To improve the numerical efficiency, an under-relaxation method with relaxation coefficient 0.75 has been used for the temperature.

With the uniform distribution of energy source, the chemical reaction rate $\dot{m}_{k,i}$ in the one-dimensional approximation to the flowfield in region II is readily obtained by division of $\dot{\omega}_f$ by the volume V. The flowfield downstream of the suppression vane is treated as a plug flow reactor in which the global reaction rate model (14) determines the combustion processes.

**Treatment of Boundary Conditions**

In order to solve this problem, boundary conditions must be specified adequately. Earlier works have shown that these conditions can be obtained by considering: 1) physical processes, 2) compatibility relations obtained from method of characteristics, and 3) numerical one-sided differences.[14,15] For gas phase, the boundaries are chosen to be the inlet throat and the entrance of the exhaust nozzle respectively. The upstream boundary conditions are determined by assuming conservation of total energy and isentropic process from the plenum chamber to the throat, together with the leftward characteristic equation or choked condition, depending on the flow speed at the throat. At the downstream end, the flow is subsonic. Two characteristic lines run from the interior region to the exit; the only physical boundary condition required comes from the Mach number at the exit. The

conditions for the liquid phase can be specified with the same procedure described in reference 15.

With the treatment of the inlet and the combustor separately, an internal boundary is introduced at the dump plane. The three compatibility relations, two in the inlet section and one in the combustor, together with the continuity equations for the mass, pressure, and total energy provide the necessary boundary conditions for the finite-difference approximation in each region.

**Numerical Scheme**

The numerical scheme originally developed for dealing with combustion instabilities in solid propellant rockets[14,16] has been extended to the present analysis. It employs a combined finite difference operation. The conventional two-step Lax-Wendroff method is hybridized with Harten and Zwas' first order scheme and further modified by an artificial compression correction.[17] Because of its remarkable feature of accommodation of steep-fronted waves, this scheme is particularly suitable for the analysis of various instability problems.

## III. DISCUSSION OF RESULTS

Calculations have been carried out for the flowfields in a research side-dump ramjet engine operated at the Naval Weapons Center.[7] The primary input data simulating a typical experiment are given in Table II.

Table 2. Computer program input parameters

| | |
|---|---|
| $T_{T_0} = 612\ K$ | $L = 350\ J/g$ |
| $p_{1.5} = 7.728\ atm$ | $\Delta H = 42397\ J/g$ |
| $\rho_{1.5} = 4.23\ Kg/m^3$ | $\rho_l = 940\ Kg/m^3$ |
| $M_{1.5} = 0.23$ | $\sigma_l = 0.023\ N/m$ |
| $T_{T_4} = 2323\ K$ | $\mu_l = 0.0035\ Ns/m^2$ |
| $M_4 = 0.37$ | $c_l = 2.1 J/g-K$ |
| $\varphi = 0.91$ | $\mu = 3\times10^{-5}\ Ns/m^2$ |
| $T_{bp} = 480K$ | $c_p = 1.05\ J/g-K$ |
| | $K = 0.046\ J/s-m-K$ |

Because the engine always exhibits oscillatory behavior, in the calculation of mean flow fields, the Mach number in the inlet section is fixed by the measured value. The requirement for the continuity of pressure across the dump plane is satisfied by choosing a suitable pre-exponential factor in the chemical reaction rate equation. For unsteady problems, the condition for a fixed inlet Mach number is relaxed. The internal boundary conditions at both sides of the dump plane are calculated, based on the model given in Sec. II.

Figure 3 summarizes the distributions of various mean flow properties. The rapid changes of the pressure and velocity downstream of the dump plane are due to combustion processes. For the conditions chosen here, most of the chemical reaction, over eighty percent, takes place in the stirred reactor section. Figure 4 shows the bulk density of the liquid fuel and the mass concentration of the fuel vapor in the inlet section. Most of the fuel is evaporized before entering the combustor. This is the basis for the assumption made earlier, i.e., single-phase reaction in the combustor. The kink on the density distribution corresponds to the position at which the liquid fuel begins to evaporate.

The stability characteristics of the engine are investigated by examining the response of the flowfield to a disturbance imposed on the mean flowfield. Figure 5 shows the time history of the pressure at the end of the inlet. The amplitude of the oscillation grows up initially, then apparently reaches a limiting value after certain time. Nonlinear effects are clear from the development of this limit cycle and from the structure of the waveform. The pressure distributions at various times within one cycle of oscillations are shown in Figure 6. A pressure node exists in the combustor, corresponding to the first mode oscillation. The acoustic field is driven by the pressure oscillations in the combustor and damped efficiently due to the propagation of waves through the upstream boundary into the plenum chamber.

Spectral analysis of pressures at various locations has been conducted. The power spectral density for the pressure at the exit plane of the inlet is shown in Figure 7. The dominant frequency is 320 Hz, compared with the measured value 295 Hz. The wide-band noise is due to the numerical noise and the transient part of the signal. Table 3 gives the calculated and the measured frequencies of oscillations.

Table 3. Calculated and measured frequencies

| *mode* | $f_{calculated}$ | $f_{measured}$ |
|---|---|---|
| *bulk* | 176 *Hz* | 130 *Hz* |
| *first* | 320 *Hz* | 295 *Hz* |
| *second* | 624 *Hz* | 590 *Hz* |

Figure 8 shows the distributions of amplitude and phase for the first mode. The smaller cross-sectional area of the inlet produces greater amplitude. As far as the absolute magnitude is concerned, the analysis underestimates the fluctuation almost by a factor of 25 percent.

## ACKNOWLEDGMENTS

The authors are indebted to Mr. J. N. Levine for providing the current numerical code for the self-adjusting hybrid scheme, and to W. H. Clark and J. W. Humphrey for several informative conversations. This work represents a part of the results obtained from the research program supported partly by the California Institute of Technology and partly by the Air Force Office of Scientific Research, Grant No. AFOSR-80-0265.

## REFERENCE

1. Waugh, R. C., et al., "Ramjet Combustor Instability Investigation: Literature Survey and Preliminary Design Study," *United Technologies Report CSD-2770-IR-1*, Jan.1982.

2. Culick, F. E. C. and Rogers, T., "Modeling of Pressure Oscillations in Ramjets," *AIAA/SAE/ASME 16th Joint Propulsion Conference*, June 1980.

3. Yang, V. and Culick, F. E. C., "Linear Theory of Pressure Oscillations in Liquid-Fueled Ramjet Engines,"

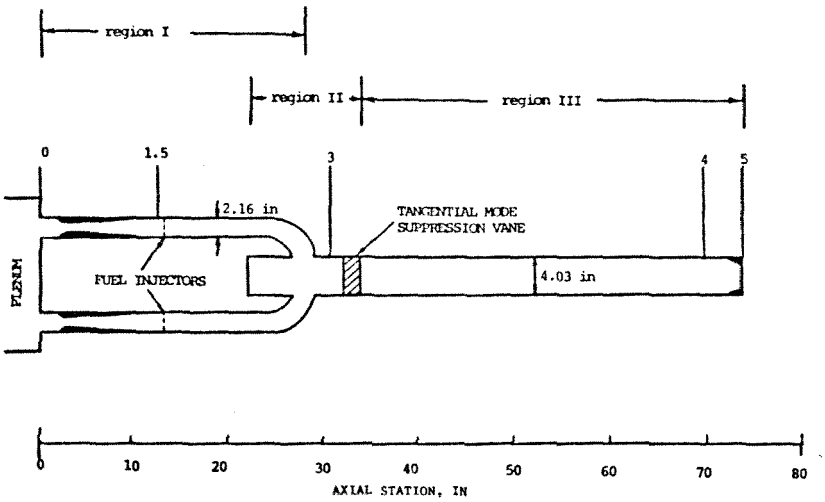


FIG. 1: BASELINE CONFIGURATION

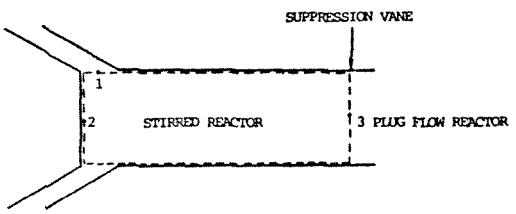


FIG. 2: SCHEMATIC DIAGRAM OF AN EQUIVALENT COMBUSTOR

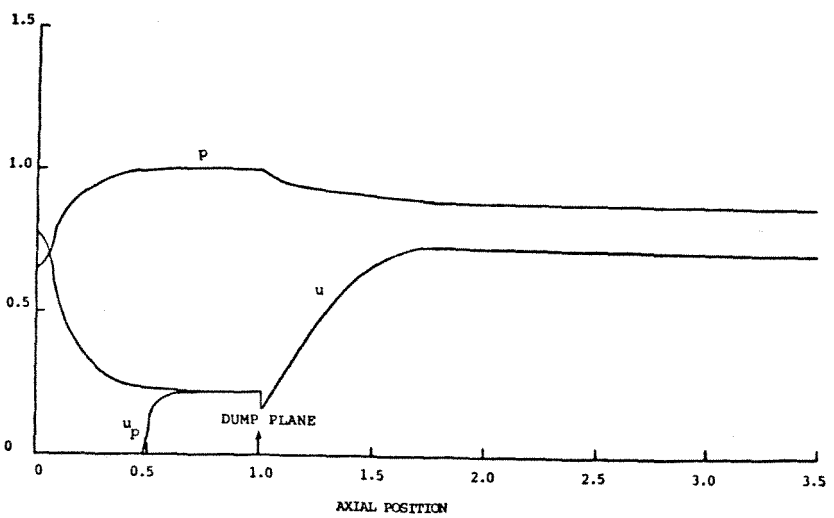


FIG. 3: DISTRIBUTIONS OF MEAN FLOW PROPERTIES

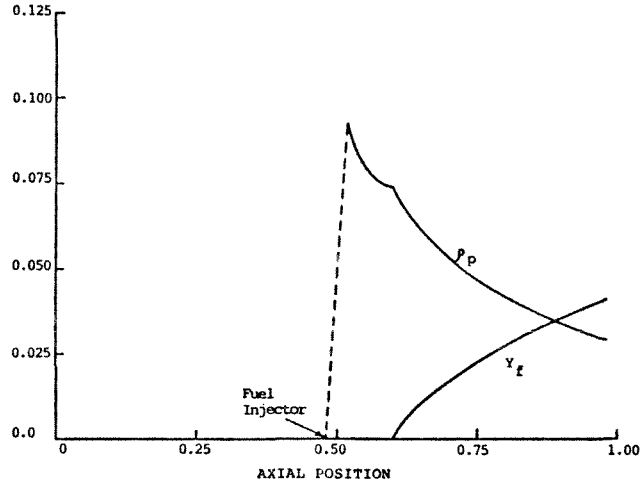


FIG. 4: DISTRIBUTIONS OF LIQUID FUEL DENSITY AND MASS CONCENTRATION OF FUEL VAPOR IN THE INLET

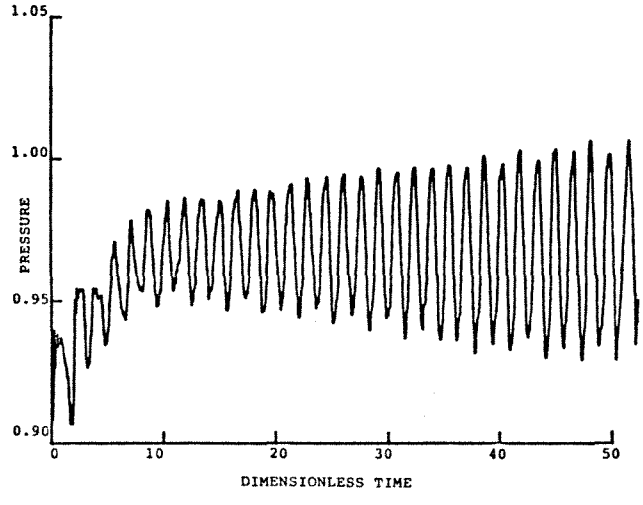


FIG. 5: TIME HISTORY OF PRESSURE AT THE END OF THE INLET

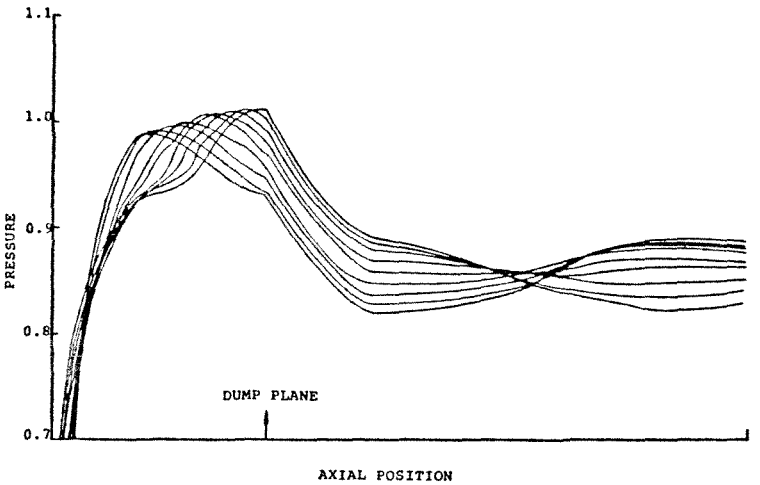


FIG. 6: PRESSURE DISTRIBUTIONS AT VARIOUS TIMES WITHIN ONE CYCLE OF OSCILLATION

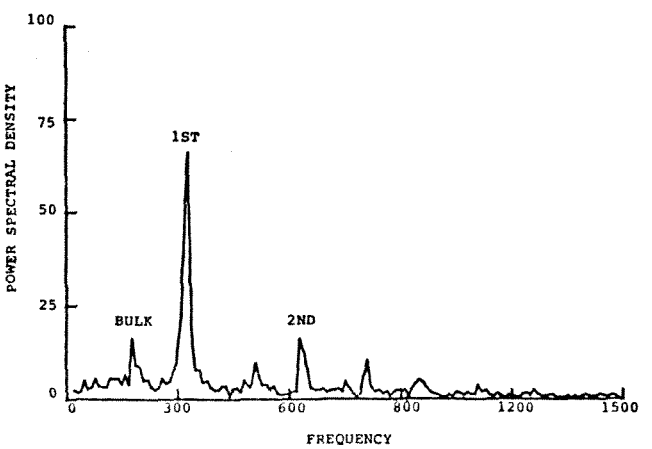


FIG. 7: POWER SPECTRAL DENSITY OF PRESSURE AT THE END OF THE INLET

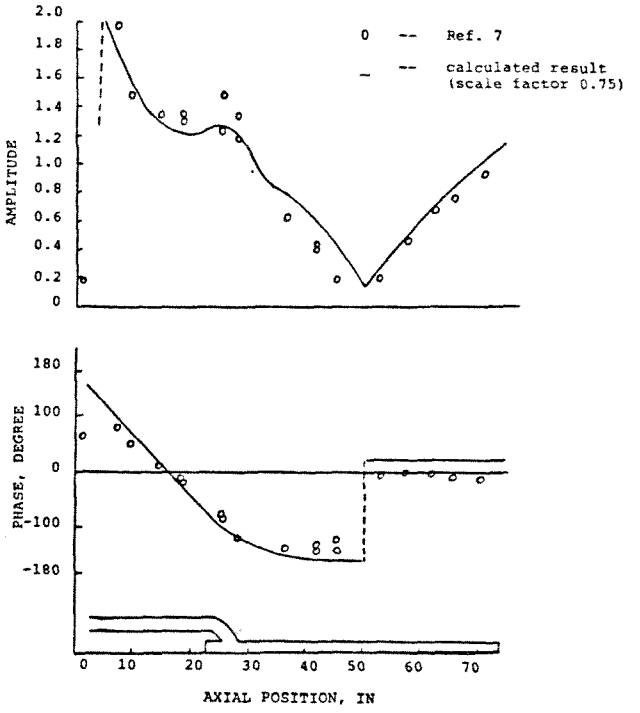


FIG. 8: DISTRIBUTIONS OF AMPLITUDE AND PHASE OF FIRST MODE OSCILLATION